Compliance of the Hair Bundle Associated with Gating of Mechanoelectrical Transduction Channels in the Bullfrog's Saccular Hair Cell

J. Howard and A. J. Hudspeth
Department of Physiology
University of California
San Francisco, California 94143-0444

Summary

Mechanical stimuli are thought to open the transduction channels of a hair cell by tensing elastic components, the gating springs, that pull directly on the channels. To test this model, we measured the stiffness of hair bundles during mechanical stimulation. A bundle's compliance increased by about 40% at the position where half of the channels opened. This we attribute to conformational changes of transduction channels as they open and close. The magnitude and displacement dependence of the gating compliance provide quantitative information about the molecular basis of mechanoelectrical transduction: the force required to open each channel, the number of transduction channels per hair cell, the stiffness of a gating spring, and the swing of a channel's gate as it opens.

Introduction

The mechanically sensitive ion channels of hair cells confer upon vertebrates sensitivity to sound, acceleration, substrate vibration, and water motion. Stimuli affect hair cells in the inner ear, as well as those in the lateral-line organs of fishes and amphibia, by imposing forces on hair bundles. Each bundle, the mechanoreceptive organelle of a hair cell, consists of some tens to hundreds of actin-filled stereocilia protruding from the apical cellular surface. Deflection of a hair bundle in the positive direction, toward the tallest stereocilia, opens transduction channels, whereas negative deflection closes them. These channels are permeable to small cations and seem to be located near the tip of the hair bundle (for reviews see Hudspeth, 1983, 1985b; Howard et al., 1988).

Several experiments suggest that the gates of the transduction channels are opened when deflection of the hair bundle tenses elastic elements, the gating springs, that pull directly on the channels (Corey and Hudspeth, 1983b; Holton and Hudspeth, 1986; Howard and Hudspeth, 1987). In the model for the gating of transduction channels portrayed in Figure 1 (Howard et al., 1988), each channel can exist in two conformations, a closed (nonconducting) state and an open (conducting) one. The opening of a channel shortens the associated gating spring by a distance that is envisioned to be of molecular dimensions; the distance might, for example, be the displacement of a protein domain that obstructs the channel only in the closed configuration. The farther the bundle is deflected in the positive direction, the greater the tension in the gating spring and the lower the energy of

the open state with respect to that of the closed; the channel is thus biased to spend more time open.

The gating-spring model is consistent with the sigmoidal dependence of the steady-state transduction current on bundle displacement (Corey and Hudspeth, 1983a; Holton and Hudspeth, 1986; Ohmori, 1987), the sub-millisecond delay between bundle displacement and channel opening (Corey and Hudspeth, 1979a, 1983b), and the dependence of the rate of gating on displacement and temperature (Corey and Hudspeth, 1983b). The correlation between adaptation of the transduction current (Eatock et al., 1987) and mechanical relaxation of the bundle suggests that adaptation is mediated by a time-dependent reduction of the tension in gating springs (Howard and Hudspeth, 1987). These springs might correspond to the filamentous links that can be seen by electron microscopy to connect the tip of each stereocilium to its tallest neighbor (Pickles et al., 1984). Such a role for the tip links would accord with the directionality of the response, the location of the channels near the tips of the stereocilia (Hudspeth, 1982), and the small number, at most 5, of transduction channels per stereocilium (Ohmori, 1984, 1987; Holton and Hudspeth, 1986).

Because mechanical energy is required for the gating of the channels, the stiffness of the hair bundle is expected to depend on the state of the channels (Howard et al., 1988). This argument may be appreciated with the aid of the model of the gating spring and transduction channel shown in Figure 1. While the channel remains either closed or open, the stiffness of the transduction apparatus is simply the stiffness of the gating spring. If the channel is allowed the freedom to move between the two states, however, the stiffness of the transduction apparatus will be less than that of the gating spring alone because of the extra give contributed by the configurational change of the channel. This model, which is quantified in Experimental Procedures, predicts that the stiffness of the hair bundle (K_B) includes the stiffness of the stereociliary pivots (K_S), the stiffness contributed by the gating springs themselves (K_G), and a term that depends upon the probability (p) of the channels' being open:

$$K_B = K_S + K_G - Nz^2 p(1 - p)/kT \qquad (1)$$

The final term, which is always negative, corresponds to a decrease in stiffness—an increase in compliance—contributed by the gating of the transduction channels. This compliance depends on the number (N) of channels, the gating force (z) for opening a single channel, Boltzmann's constant (k), and the absolute temperature (T). The steady-state probability of the channels' being open is a sigmoidal function of bundle displacement (X) and of the single-channel gating force:

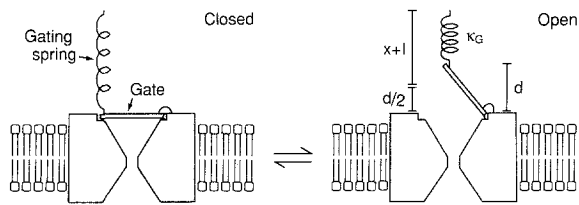$$p = \{1 + \exp[-z (X - X_0)/kT]\}^{-1} \qquad (2)$$

Figure 1. A Model for the Transduction Element of a Hair Cell

The conductance of a transduction channel is regulated by a molecular gate that can assume only two positions, open and closed. Positive displacement of the hair bundle increases the tension in the gating spring, of stiffness κ_G, which is attached to the gate. When the channel is closed, the spring is extended by a distance $x + d/2$ beyond its natural length, l. Opening of the channel shortens the spring by a distance d (right). The gating springs may be the extracellular filaments seen by electron microscopy to connect neighboring stereocilia at their tips.

X_0 is the displacement at which half the channels are open. At this position the model predicts that the bundle's stiffness should decrease by $Nz^2/4kT$ from the level of $K_G + K_S$ attained with the bundle extensively deflected in either the positive or the negative direction.

In this paper we report experiments designed to detect the hair-bundle compliance associated with the gating of transduction channels. While making mechanical measurements, we simultaneously recorded receptor potentials to assay the proportion of channels opened by each stimulus. The results lend qualitative support to the gating-spring model and provide values for several molecular properties of the transduction apparatus.

Results

Mechanical and Electrical Response

The tip of a flexible glass fiber was attached to the bulbous tip of the kinocilium in a hair bundle (Figure 2A), and the base of the fiber was then moved by a piezoelectrical stimulator through steps of various amplitudes and directions. Because the glass fiber's stiffness was comparable to that of the hair bundle, movement of the fiber's base resulted in both displacement of the bundle's tip and flexion of the fiber (Figure 2B). The motion of the fiber's tip was measured optically with a photodiode sensor. The difference between this motion and the displacement imposed at the fiber's base was the flexion of the fiber; the force exerted on the bundle was the product of this flexion and the fiber's calibrated stiffness. The bundle's stiffness could then be calculated as the ratio of the force on the bundle to the extent of its deflection at any time (Flock and Strelioff, 1984; Crawford and Fettiplace, 1985; Howard and Ashmore, 1986; Howard and Hudspeth, 1987).

When a force of about 70 pN was applied to a hair bundle bathed in the standard saline solution, a complex mechanical and electrical response ensued (Figure 3A). This bundle rapidly moved a distance of 74 nm; then, after a transient reversal of its direction of motion, or rebound, the bundle relaxed to a steady-state position
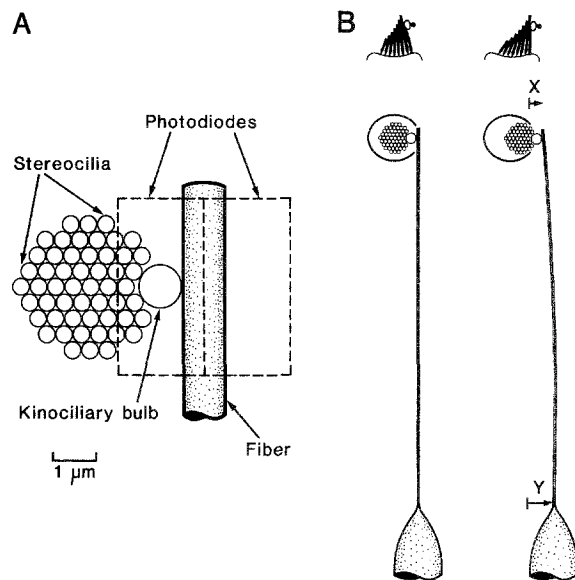

Figure 2. Technique for the Measurement of Hair-Bundle Stiffness

(A) A hair cell from the bullfrog's sacculus was stimulated by displacement of a fine glass fiber adhering to the bulbous tip of the kinocilium in the hair bundle, about 6.7 μm above the bundle's base. A magnified image of the fiber's tip was projected onto a photodiode pair; the relation between the image and the photodiodes is indicated schematically.

(B) Displacement of the fiber's base by a distance Y deflected the bundle by a distance X from its resting position; the extent to which the calibrated fiber was bent $(Y - X)$ provided a measure of the force exerted on the bundle. The hair bundle is shown both in a top view (lower) and in profile (upper); for illustrative purposes, the fiber's length has been diminished and the bundle's deflection exaggerated.

with a time constant of 31 ms. At the conclusion of the force pulse, the bundle displayed a rapid displacement step, then relaxed more slowly to its resting position with a time constant of 43 ms.

Simultaneous recordings of membrane potential with a single microelectrode demonstrated a depolarizing receptor potential that rose rapidly during the bundle's initial displacement, then fell to a smaller, steady-state depolarization (Figure 3A). The rapid decline following the peak receptor potential may be associated with the bundle's rebound, while the slower component has a time constant similar to that of the bundle's mechanical relaxation. The response at the termination of the stimulus included a rapid repolarization followed by slower adaptation toward the resting potential. The temporal correspondence between the bundle's mechanical relaxation and adaptation of the cell's electrical response led us to propose that adaptation is mediated by reduction of the tension in a component of the hair bundle that pulls on the channels (Howard and Hudspeth, 1987). In this paper we are chiefly concerned with the gating of transduction channels rather than their adaptation, and hence with mechanoelectrical events occurring on a time scale of milliseconds rather than tens of milliseconds.

A

C

Bundle Stiffness (μN·m^{-1})

2000

1000

-100   0   100

Displacement (nm)

B

D

Receptor Potential (mV)

12

8

4
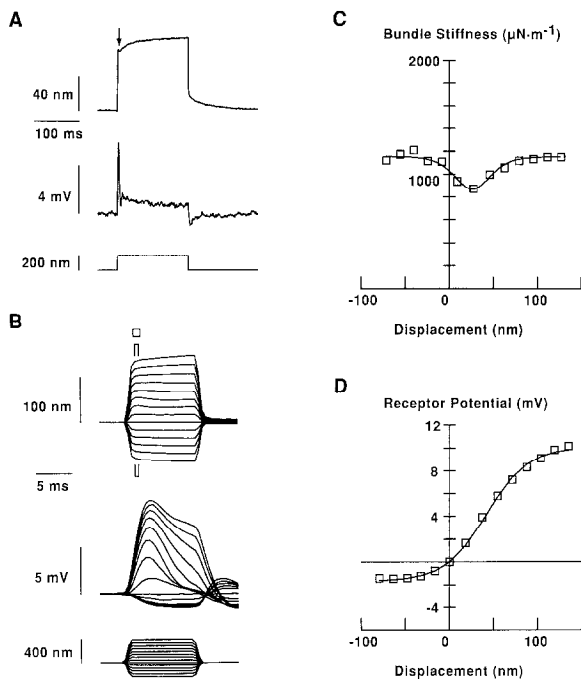
-4

-100   0   100

Displacement (nm)

Figure 3. Demonstration of the Gating Compliance

(A) A hair bundle was stimulated in standard saline solution by a displacement pulse administered to the base of a stimulus fiber (bottom trace). After a rapid response, the bundle's displacement (top trace) displayed a transient rebound (arrow) and a slower relaxation; a relaxation in the opposite direction was also evident following the termination of the force pulse. After a rapid transient associated with the rebound, the cell's receptor potential (middle trace) adapted with a time course similar to that of the bundle's mechanical relaxation.

(B) Families of bundle displacements (top traces) and receptor potentials (middle traces) recorded from the same cell during stimulation with fiber displacements of various amplitudes (bottom traces). Note the change in time scale.

(C) A plot of the instantaneous stiffness of the bundle (squares) as a function of displacement. The data were taken from the records in (B) during the time interval indicated by the brackets above and below the bundle-displacement traces. The theoretical relation derived from the gating-spring model is shown for comparison (continuous curve); z = 293 fN; X_0 = 26 nm; N = 54.

(D) A plot of the peak receptor potential (squares) as a function of displacement; the gating-spring model's prediction for this relation, a Boltzmann curve, is also indicated (continuous curve); z = 170 fN; X_0 = 42 nm. The cell's resting potential was −61 mV, and the fiber's stiffness was 535 μN·m^{-1}; 64 records were averaged to produce the traces shown in (B).

Gating Compliance

To determine the bundle's stiffness as a function of displacement, we obtained mechanical responses for positive and negative mechanical stimuli of various amplitudes (Figure 3B). In most instances, measurements were made in the interval 0.75–1.25 ms after the fiber's base was moved. Two factors dictated this choice for the measurement interval. First, the two time-dependent phenomena discussed above, the rapid rebound and the slower, exponential relaxation, provided a complication that could be circumvented by measuring the bundle's

stiffness no later than 1.25 ms after the onset of a force step. Second, the stimulus fibers and the hair bundle experience viscous drag from the surrounding fluid. The fibers were manufactured to be sufficiently short, 100–200 μm, so that they did not significantly load the bundle hydrodynamically. When attached to a bundle, the tip's time constant of approach to a new position was about 250 μs (Experimental Procedures); we therefore made stiffness measurements no sooner than 750 μs after the onset of stimulation. Because the rate constants for channel opening and closing are about 100 μs at room temperature (Corey and Hudspeth, 1983b), each channel's probability of being open was essentially in equilibrium with the bundle's position. Hydrodynamic drag precluded our resolving mechanically the time course of channel opening; the stiffness instead depended on the steady-state probability of the channel's being open, and Equation 2 applies.

When determined 0.75–1.25 ms after the onset of a force step, the bundle's stiffness depended on its position (Figure 3C). As predicted by the gating-spring model (Equation 1), the stiffness was smaller over a roughly 125 nm range of displacements and was minimal at a displacement 26 nm positive to the bundle's resting position. For the cell whose responses are illustrated, the bundle's minimal stiffness was 290 μN·m^{-1} smaller than the stiffness of 1150 μN·m^{-1} measured immediately after the bundle was pushed more than 50 nm in the negative direction or more than 75 nm in the positive direction. The displacement dependence of this bundle's stiffness fit well with the theoretical prediction of the gating-spring model with 54 channels (Equation 1; Figure 3C).

Similar mechanical recordings were obtained from a total of 34 cells studied 0.75–1.25 ms after the onset of fiber deflection. The bundles' average stiffness declined to a minimum 390 ± 240 μN·m^{-1} (mean ± SD; range 150–1100 μN·m^{-1}) less than the stiffness measured at large negative or positive displacements, 930 ± 370 μN·m^{-1} (mean ± SD; range 490–2080 μN·m^{-1}). The greatest compliance occurred at a deflection of 22 ± 12 nm (mean ± SD; range −24 to 43 nm) from the bundle's resting position.

The displacement dependence of the peak of the simultaneously recorded receptor potential (Figure 3B) indicated that the transducer was most sensitive over the range of deflections for which the bundle was least stiff (Figure 3D). The displacement at which the peak receptor potential reached its half-maximal value was 42 nm; the 16 nm by which this differed from the point of minimal stiffness was only about 10% of the transducer's operating range. To determine approximately the range of displacements over which the transducer was most sensitive, we fitted the gating-spring model's prediction for the transduction current as a function of displacement, a Boltzmann relation (Equation 2), to the peak values of the receptor potential (Figure 3D). This fit was satisfactory and provided an estimate of the single-channel gating force, 170 fN, comparable to the value

of 290 fN determined by fitting the theory to the stiffness data from the same cell.

In simultaneous mechanical and receptor potential recordings from 22 cells, the position of the bundle's greatest compliance coincided closely with the position at which the peak of the receptor potential reached half its maximal value: on average, the bundle's maximal compliance lay only 10 ± 13 nm (mean ± SD) negative to the half-amplitude point on the relation between peak receptor potential and displacement. This result is consistent with the hypothesis that the bundle's increase in compliance is associated with the gating of transduction channels. Further support for this hypothesis is the overlap between the range of displacements in which the compliance increases and the slightly broader range of the receptor potential. The single-channel gating force (z) which determines the displacement ranges of both the stiffness and the receptor potential data, was 290 ± 60 fN (mean ± SD) for the former and 180 ± 50 fN (mean ± SD) for the latter. We conclude that the hair bundle exhibits additional compliance, which we call the gating compliance, over the range of displacements in which the receptor potential is changing, and hence in which the gating of transduction channels occurs.

Although the stiffnesses of bundles cited above were measured approximately 1 ms after deflection of the stimulating fiber, the gating compliance was not restricted to this particular time. Some cells did not display a rebound or adaptation, or lost them during protracted recording. For example, after more than 500 s of recording, the cell whose responses are shown in Figure 4A lost its rebound and adaptation of the receptor potential became very slow. Gating compliance was demonstrable throughout the mechanical responses (Figure 4B), and the position of minimal stiffness coincided with the position of the transducer's greatest sensitivity (Figure 4C).

Lowering the extracellular Ca^{2+} concentration slowed both the rebound and the adaptation. When the extracellular Ca^{2+} concentration was reduced to 300 μM, similar to that in the endolymph of the bullfrog's sacculus (A. J. H. and R. A. Jacobs, unpublished observations), the rebound was absent or too slow to be resolved. Al-

though microelectrode recordings were difficult to obtain in cells bathed in such low Ca^{2+} solutions, mechanical measurements demonstrated the gating compliance throughout the duration of the stimuli. Even in the standard, 4 mM Ca^{2+} saline solution, the few cells that displayed no rebound manifested the gating compliance throughout the mechanical response. We observed an increase in bundle compliance at the position of maximal sensitivity in extracellular solutions with various Ca^{2+} concentrations: the 34 cells for which the detailed analysis above was performed included 21 in 4 mM Ca^{2+}; 2 in 2 mM Ca^{2+}; 9 in 1 mM Ca^{2+}; and 2 in 300–500 μM Ca^{2+}. The magnitude and the spatial extent of the gating compliance did not depend significantly on the extracellular Ca^{2+} concentration.

Adaptation

Hair cells of the bullfrog's sacculus adapt to constant stimuli: in response to a maintained deflection, the range of positions in which the hair bundle is sensitive shifts to accord with the new holding position (Eatock et al., 1987). If the compliance that we have measured arises from flexion of passive components of the hair bundle, for example the actin of the stereocilia, it would be expected to be independent of adaptation. If on the other hand the gating-spring model is correct, then the position of the bundle's increased compliance should shift with the region of mechanosensitivity.

Our results accorded with the gating-spring model. After measuring the mechanical and electrical responses of a hair cell, we subjected its hair bundle to a sustained, positive force and delivered similar stimuli about the new resting position. The bundle was then subjected to a negative force, and identical stimuli were delivered. The relation between stiffness and displacement changed pari passu with that between receptor potential and displacement: the bundle's position of least stiffness changed as the transducer adapted (Figures 5A and 5B). Similar results were obtained from 10 additional cells. When hair bundles were subjected to steady forces that produced positive and negative offsets, both the positions of greatest compliance and the positions at which
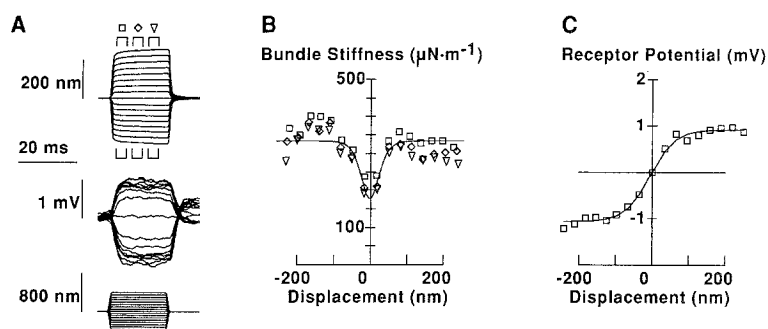

Figure 4. Gating Compliance without Response Transients

(A) Records of a hair bundle's displacement (top trace) and of the simultaneously measured receptor potential (middle trace) were obtained in 1 mM Ca^{2+} saline solution from a cell without a rebound and with slow adaptation. The cell's resting potential was −35 mV; 32 traces were averaged.

(B) Plots of the instantaneous stiffness of the hair bundle, taken at the 3 times indicated above and below the mechanical records in (A). The data indicate that the gating compliance was essentially constant in amplitude and position throughout the response to mechanical stimulation.

(C) A plot of the receptor potential's peak as a function of displacement, constructed from the families of records shown in (A). The bundle's stiffness was minimal at the displacement for which the transducer was most sensitive. The continuous curve in the stiffness plot was produced with $z = 243$ fN; $X_0 = -2$ nm; N = 42; the curve in the receptor–potential trace corresponded to $z = 122$ fN; $X_0 = -7$ nm.

A   Bundle Stiffness (μN·m^{-1})
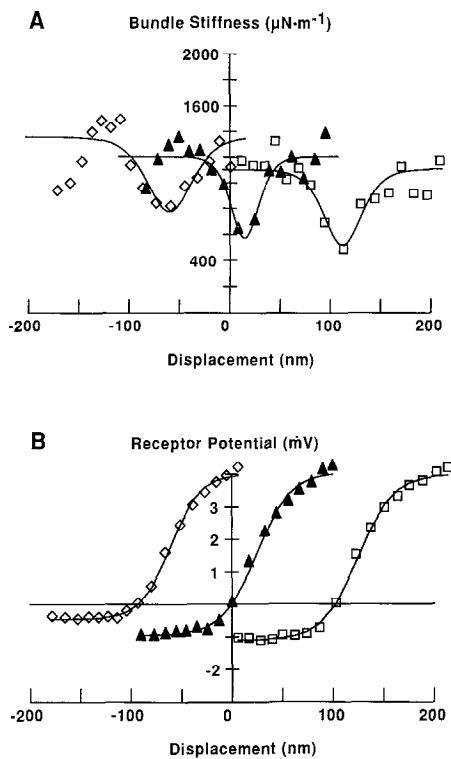

B   Receptor Potential (mV)

Figure 5. Shift of the Position of the Gating Compliance with Mechanosensitivity during Adaptation of the Transducer

(A) A hair cell was stimulated by a family of force pulses to the hair bundle's tip; the experiment was then repeated while the bundle was offset by positively or negatively directed stimuli that respectively produced steady displacements of 103 nm and −93 nm. The plots of bundle stiffness against displacement demonstrate that the gating compliance changes its position during adaptation of the mechanoelectrical transducer.

(B) The relation between bundle displacement and the receptor potential measured simultaneously with the data of (A) indicates that the shift of the gating compliance matches the extent of transducer adaptation. The resting potential of this cell, which was bathed in 1 mM Ca^{2+} saline, was −45 mV. The values used to generate the theoretical stiffness curves were, from left to right: $z = 236$ fN, $X_0 = -61$ nm, $N = 167$; $z = 428$ fN, $X_0 = 15$ nm, $N = 55$; and $z = 314$ fN, $X_0 = 113$ nm, $N = 95$. The continuous curves in (B) were generated with: $z = 269$ fN, $X_0 = -61$ nm; $z = 234$ fN, $X_0 = 25$ nm; and $z = 231$ fN, $X_0 = 125$ nm.

the peak receptor potentials reached their half-maximal values closely followed the offset displacements. The transducer could adapt almost completely to displacements up to 300 nm in either direction; for the 11 cells studied, the mechanical and electrical results respectively indicated that adaptation proceeds to an extent 95% ± 2% and 92% ± 2% (mean ± SE) of the magnitude of the bundle's static offset.

Gentamicin

Aminoglycoside antibiotics applied extracellularly to the apical surfaces of hair cells prevent the transduction current from being modulated by movement of the hair bundle. The effect of these ototoxic drugs is greatest when a hair cell's membrane is hyperpolarized and be-

comes progressively less as the cell is depolarized (Ohmori, 1985). The drugs are cationic and probably interact with a negatively charged binding site in or near the membrane; the simplest hypothesis is that the binding site lies inside the pore and that occupation of this site blocks the flow of ionic current through the channel (Howard et al., 1988).

To test the possibility that aminoglycoside antibiotics also affect the channel's gating, we made mechanical recordings before, during, and after exposure of hair bundles to a bathing solution containing 100 μM gentamicin. This concentration is sufficient to reduce the transduction current to about 20% of its control value. Gentamicin rendered the bundle's stiffness independent of position: it abolished the position-dependent compliance (Figure 6). The effect was reversible; after the preparation was superfused by control solution, the stiffness again manifested its characteristic displacement dependence. Similar results were obtained from 4 other cells. Gentamicin thus interferes reversibly with channel gating, nullifying the compliance associated with gating of transduction channels. Gentamicin's abolition of the gating compliance suggests that, while occluding a pore, a drug molecule additionally restricts the opening and closing of the channel's molecular gate.

Discussion

Gating Is Mediated by Elastic Elements

The stiffness of a hair bundle is greatest for substantial positive and negative displacements. Over the intervening range of deflections, near the bundle's resting position, the bundle's stiffness is less: its compliance is greater. Simultaneous measurements of the receptor potential indicate that the bundle is more compliant over the range of displacements in which the transducer is more sensitive; the compliance is greatest when about half the channels are open. Both the position of maximal compliance and the position of greatest sensitivity of the transducer shift as the transduction apparatus adapts to sustained stimuli. While blocking the receptor potential, gentamicin reversibly renders the bundle's stiffness independent of position. Because these various results all indicate that the bundle's increase in compliance is associated with the opening and closing of transduction channels, we term the phenomenon the gating compliance.

We believe that the gating compliance is a manifestation of the gating of transduction channels. To reach this conclusion, however, we must exclude explanations for the bundle's increase in compliance that are unrelated to transduction or that arise from events subsequent to the gating of transduction channels.

It is conceivable that the compliance is caused by nonlinear mechanical properties of the bundle that are not directly involved with the gating of transduction channels. The bundle might, for example, exhibit a reduced stiffness over a range of deflections in which the connections between adjacent stereocilia are slack. Until this slack was taken up, a positively directed stimulus
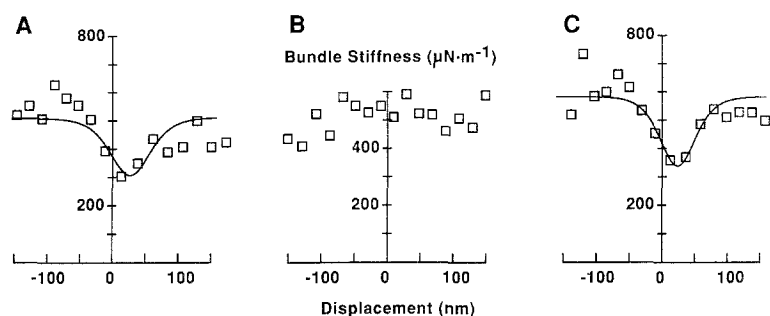
Figure 6. Blockade of the Gating Compliance by an Aminoglycoside Drug

(A) The relation between instantaneous bundle stiffness and displacement was measured under control conditions in a saline solution containing 4 mM Ca^{2+}. (B) The gating compliance disappeared when the hair bundle was bathed in a similar solution containing 100 μM gentamicin, an ototoxic antibiotic that interferes with transduction. (C) The gating compliance returned with the restoration of standard saline solution. The theoretical curve in (A) was produced with z = 193 fN, X_0 = 27 nm, N = 87; the curve in (C) corresponds to z = 219 fN, X_0 = 23 nm, N = 81.

would deflect, not the entire bundle, but only a limited number of stereocilia. If this were the case, however, it is difficult to understand why transduction, which presumably involves deflection of all the stereocilia, is most sensitive near the bundle's resting position. In addition, the migration of the bundle's position of maximal compliance during adaptation and gentamicin's blockade of the gating compliance cannot readily be explained by the hypothesis of slack connections between stereocilia.

Another possibility is that the gating compliance is caused by events subsequent to the opening and closing of transduction channels; Ca^{2+} entry into the stereocilia through the channels or changes in membrane potential might somehow affect stereociliary stiffness. Because the stiffness is maximal when the channels are either fully open or fully closed, it would have to be supposed that the hypothetical subsequent events have a nonmonotonic dependence on the probability of the channels' being open. Moreover, in both its displacement dependence and its magnitude, the gating compliance is independent of the extracellular Ca^{2+} concentration; such an effect of Ca^{2+} entry on bundle stiffness is therefore improbable. Furthermore, the gating compliance is detectable as early as 250 μs after the onset of the mechanical stimulus, well before the receptor potential has reached its peak (Figure 3B) and within a fraction of a millisecond of when the receptor current peaks (Howard and Hudspeth, 1987). It is therefore unlikely that the compliance increase is a consequence of membrane depolarization; this accords with our measurement of the gating compliance over a large range of resting potentials.

The data thus support the fundamental hypothesis underlying the gating-spring model: gating of the transduction channels is mediated by tension in elastic elements that pull on the channels (Corey and Hudspeth, 1983b; Howard et al., 1988). The gating-spring model was originally based upon the short latency of the transduction process in hair cells (Corey and Hudspeth, 1979a) and upon the relation between hair-bundle displacement and the resultant response (Corey and Hudspeth, 1983b; Holton and Hudspeth, 1986). By providing evidence for a direct linkage between the stereocilia and the trans-

duction channels, the observation of the gating compliance significantly buttresses the model.

The present experiments are the first to measure directly the stiffness contributed by the hair cell's transduction channel, or indeed by any ion channel. The recordings are related to measurements of the gating current associated with voltage-sensitive channels (Armstrong and Bezanilla, 1974): both measurements involve detection of the work done on a molecular gate by an applied force, either mechanical or electrical. Gating charge is detected through a nonlinearity in the relation between the transmembrane potential and the charge stored by the membrane; that is, as an increase in the membrane's capacitance conferred by the rearrangement of charge within channel molecules over a certain range of membrane potentials. The gating compliance similarly represents a nonlinearity in the relation between force and hair-bundle displacement over a particular range of bundle positions.

The compliance that we have measured differs from the previously reported, apparently monotonic decrease in stiffness upon deflection of bundles in the negative direction (Flock and Strelioff, 1984). We found instead a nonmonotonic decrease in bundle stiffness whose magnitude is usually greatest on positive stimulation. The earlier result may correspond to the marked diminution in bundle stiffness that we occasionally observed with large negative stimuli (Figure 5A, leftmost trace). It is possible that this stiffness decrease is caused by an artifact in the coupling between the fiber and bundle or by a different mode of motion of the bundle, such as torsion. It is tempting to speculate, however, that the stiffness reduction results from slackening of the gating springs.

Single-Channel Gating Force

The bundle's experimentally determined stiffness is adequately fitted by Equation 1, derived from the gating-spring model. When a Boltzmann relation (Equation 2), the model's prediction for the value of the steady-state transduction current, is applied to the relation between displacement and the peak of the receptor potential, a satisfactory fit is also obtained. The range of displace-

ments over which the compliance increases is, however, narrower than the range over which the mechanoelectrical transducer is sensitive. The single-channel gating force deduced from the stiffness, 290 ± 60 fN (mean ± SD; N = 22; range 200–400 fN), is accordingly somewhat larger than that inferred from the receptor potential measured in the same cells, 180 ± 50 fN (mean ± SD; range 95–290 fN). Because measurements of the receptor potential are distorted by the membrane's time constant, by electrical rectification in the hair cell's membrane, and by changes in the driving force for the transduction current (Corey and Hudspeth, 1979b), voltage-clamp measurements of the receptor current must be performed to establish whether the disparity is significant.

The single-channel gating force, the difference between the force exerted on the fiber by a transduction channel when it is open and that exerted when it is closed (Hudspeth, 1985a), is about an order of magnitude smaller than the force thought to be produced in muscle as a consequence of the hydrolysis of a single molecule of ATP by the actin–myosin reaction (Huxley and Simmons, 1971). It should be noted that the gating compliance is the derivative of a nonlinear force that depends on the state of the transduction channels (Equation 10). This force is analogous to the component of tension that depends on the configuration of myosin molecules following isometric contraction of a muscle fiber (Huxley and Simmons, 1971).

It is unclear how many states the hair cell's transduction channels can occupy (Corey and Hudspeth, 1983b; Holton and Hudspeth, 1986). The kinetic behavior of channel gating measured from the bullfrog's saccular epithelium (Corey and Hudspeth, 1983b) and the asymmetry of the relation between the steady-state current and displacement (Corey and Hudspeth, 1983a; Ohmori, 1987) both suggest that the channels have more than two states. If this were the case, we would expect that part of the gating compliance would correspond to transitions among closed states, or among open states, of the channel. Because the range of the gating compliance and that of channel opening largely overlap, however, we infer that the bundle's increase in compliance is largely influenced by the transitions between just two states. Large positive or negative deflections respectively open or close all the transduction channels (Holton and Hudspeth, 1986); we therefore conclude that the displacement-sensitive transitions occur between a closed and an open state of the channel.

Number of Transduction Channels
The magnitude of the gating compliance may be used with the gating-spring theory to estimate the number of functional transduction channels per hair cell. The data indicate that the number of transduction channels in each bundle is 85 ± 45 (mean ± SD; N = 34; range 33–220). If they are distributed evenly throughout the bundle, the channels would thus number about 1–3 on each of the roughly 50 stereocilia. The present estimate

is within the range of 1–5 channels per stereocilium obtained from analysis of the transduction currents of bullfrog saccular hair cells (Holton and Hudspeth, 1986) and chick vestibular hair cells (Ohmori, 1984, 1987).

If each gating spring were to pull on 2 channels, 1 at each end, then the gating of the 2 channels would display negative cooperativity: the opening of 1 channel would favor the closing of the other. The relation between stiffness and displacement and that between transduction current and displacement would then differ from those predicted by Equations 1 and 2; the expected difference is too small, however, to be resolved in the present data. If each gating spring has a channel at each end, the results are consistent with the presence of about 20 gating springs and 40 channels.

A large hair cell from the bullfrog's sacculus has about 50 tip links. Consistent with the hypothesis that the gating springs are the tip links, our mechanical measurements demonstrate about 85 transduction channels. If the springs are the tip links, we are unable to decide whether each link pulls on 2 channels or on only 1; the model predicts somewhat too few springs in the former case and somewhat too many in the latter.

Desensitization and Rebound
The present observations provide evidence for rapid desensitization of the transduction process in the hair cell. When a cell is stimulated by the application of a small, positive force step to its hair bundle, the receptor potential rises rapidly to a peak, then declines to a lower level. Because a similar transient in the receptor current occurs under voltage-clamp conditions (Howard and Hudspeth, 1987), this behavior is not due to the activation of the voltage- and ion-sensitive conductances in the membrane (Lewis and Hudspeth, 1983).

Desensitization may explain the discrepancy between the single-channel gating force determined in this study and that deduced in an earlier investigation of saccular hair cells using the whole-cell, tight-seal recording technique (Holton and Hudspeth, 1986). The peak probability of the channels' being open increased from 10% to 90% over a 100 nm range of displacements in the present study as compared with a 400 nm range in the previous investigation. The hair bundles in the earlier study were stimulated with a continuous, sinusoidal, ±0.5 μm displacement. It is likely that this large, repetitive stimulation desensitized the transduction mechanism, leaving the channels in a partially inactivated state.

The hair bundle's rebound movement following a rapid, positive force step is temporally associated with desensitization. If the reduction in receptor current following the transient peak is caused by the time-dependent closure of transduction channels, this closure should exert a force on the gating springs that in turn is transmitted to the entire bundle. This force would move the bundle in the negative direction, giving rise to the rebound's falling phase. The amplitude of the rebound is quantitatively consistent with this proposed mechanism: following the onset of a small, positive stimulus, the stiffness

measured just after the rebound has the high value expected if the probability of the channels' being open has decreased to near that prior to stimulation.

Our failure to observe the rebound in solutions with a low Ca^{2+} concentration, or in response to negatively directed stimuli, is consistent with the notion that the rebound is caused by Ca^{2+} entering through the channels and closing their gates. Such a role of Ca^{2+} also accords with the requirement for energy to drive the rebound. Because the rebound is a movement of the bundle in the direction opposite to the force exerted by the fiber, energy is required; this energy could come from the transmembrane electrochemical gradient for Ca^{2+}.

The rebound is of interest in the light of evidence that mechanical activity by hair cells can enhance their sensitivity to stimulation (for review see Hudspeth, 1985b). The process that produces the rebound could contribute to the exertion of forces by hair bundles. If, for example, Ca^{2+} enters through transduction channels and binds to an internal site that affects the probability of the channels being open, the resultant bundle movement would provide mechanical feedback following bundle deflection. Such a mechanism might underlie the spontaneous and evoked oscillatory motions of certain hair bundles (Crawford and Fettiplace, 1985; Howard and Hudspeth, 1987). The rate at which feedback would occur would not be limited by the membrane's time constant, but would depend instead on the rate of Ca^{2+} binding and unbinding from its site of action. Such a system might assist tuning by hair cells at much higher frequencies than can be achieved, for example, by an electrical resonance dependent upon changes in membrane potential.

Stiffness of the Gating Springs

A previous investigation of mechanical relaxation in the transduction mechanism indicated that the gating springs contribute about half of the bundle's stiffness (Howard and Hudspeth, 1987). This conclusion is supported by our present results. If the gating springs contribute the difference between the bundle's total stiffness immediately following a force step (K_B, 930 ± 370 $\mu N \cdot m^{-1}$, N = 34) and the steady-state stiffness measured at the end of a long, small stimulus (K_S, 440 ± 190 $\mu N \cdot m^{-1}$; N = 34), then K_G is approximately 500 $\mu N \cdot m^{-1}$. This result indicates that mechanoelectrical transduction by hair cells is quite efficient: about half of the mechanical work done in moving the hair bundle is directed toward gating of the mechanically sensitive channels.

Because the stiffness contributed by N gating springs is $N\kappa_G\gamma^2$ (Equation 11), the stiffness of an individual gating spring (κ_G) can be deduced if the lever ratio (γ) between bundle displacement and extension of the gating spring is known. If the tip links are the gating springs, this ratio is about 0.14 for the hair cells under investigation (Howard et al., 1988); each of 50 gating elements would then have a spring constant of about 500 $\mu N \cdot m^{-1}$. From transmission electron microscopy, the tip links are 5 nm filaments about 150 nm long (Pickles et al., 1984; A. J. H.

and R. A. Jacobs, unpublished observations). To possess the required stiffness, each of 50 filaments must have a Young's modulus of about 4 MPa. Because the bundle's tip can be displaced in excess of 1 μm without damaging the transduction apparatus (Hudspeth and Corey, 1977), a tip link must be able to withstand an elongation of at least 100%. Such a modulus and elongation are characteristic of rubber and of resilient, filamentous proteins such as elastin (Burton, 1954; Gotte et al., 1974). The argument that the tip links are the gating springs is reinforced by the observation that the instantaneous stiffness of the bundle drops sharply at the largest negative displacements (Figure 5A); perhaps the slender filaments buckle under compression.

The Swing of the Channel's Gate

The single-channel gating force (z) is given by $\kappa_G d\gamma$, the product of the stiffness of a gating spring, the distance (d) by which opening of the channel shortens the spring, and the lever ratio (Experimental Procedures). If tip links gate the channels, our data indicate that the opening swing of each of 50 channels' gates is 4 ± 2 nm (mean ± SD; N = 34). Although such a movement would represent a large change in protein conformation, it is of the same magnitude as the motion of a myosin molecule during the force step in muscle (4–8 nm; Huxley and Simmons, 1971; Ford et al., 1981). Because the channel protein has an ion-passing pore about 0.7 nm in diameter (Corey and Hudspeth, 1979b; Ohmori, 1985), this conformational change would easily suffice to open the gate.

Reciprocity

The gating-spring model involves a mechanical linkage between the stereocilia of the hair bundle and the molecular gates of the transduction channels. Such a direct connection is inherently reciprocal: not only does the application of a force to the bundle influence the distribution of open and closed channels, but the opening and closing of channels can also exert force on the bundle. A thermodynamically reversible mechanism of this sort may be contrasted with signaling via a second messenger, in which case the opening and closing of channels under the influence of varying concentrations of the messenger is not expected to exert a retrograde effect on the enzyme that generates the messenger.

The gating compliance is a manifestation of reciprocity; the mechanical impedance of the hair bundles, and presumably of the organs that contain them, depends on the state of the channels. A corollary of reciprocity is the possibility that, when stimulated by force, the transduction apparatus uses energy from ionic concentration gradients to actively move hair bundles and the structures attached to them. Such mechanical feedback would be analogous to the electrical feedback provided by the voltage-dependent sodium channels involved in the action potential; in that instance, depolarization promotes channel opening, which in turn leads to current flow and to a further depolarization. The transduction ele-

ments may prove to be more than just passive reporters of applied stimuli: if gating is also voltage- or ion-dependent, the transduction elements may be power amplifiers that participate actively in transduction and frequency selectivity.

Experimental Procedures

Theoretical Basis for the Gating Compliance

Figure 1 shows the essential features of the gating-spring model for regulation of a mechanoreceptive channel (Corey and Hudspeth, 1983b; Hudspeth, 1985a, 1985b; Howard et al., 1988). The transduction channel is connected to an elastic element, the gating spring, which is tensed by displacement of the hair bundle in the positive direction. The channel can exist in two conformations, a closed or nonconducting state and an open or conducting one; the length of the spring is greater in the former than in the latter configuration.

Suppose that the gating spring has a stiffness κ_G and that the difference in length between the open and closed states, the swing of the channel's gate, is d. When the channel is closed, the energy of the transduction element comprising the spring and channel is

$$g_c^0 = \tfrac{1}{2}\kappa_G(x + d/2)^2 + \mu_c^0 \tag{3}$$

μ_c^0 is the molecular free energy of the closed channel with no tension in the spring. At a given displacement of the hair bundle, x is the extension of the gating spring when the channel is midway between its open and closed states. The energy of the open state is

$$g_o^0 = \tfrac{1}{2}\kappa_G(x - d/2)^2 + \mu_o^0 \tag{4}$$

in which μ_o^0 is the molecular free energy of the open channel with a relaxed spring. The energy difference between the open and closed states is

$$\Delta g^0 = g_o^0 - g_c^0 = -\kappa_G dx + \mu_o^0 - \mu_c^0 \tag{5}$$

The probability (p) of finding the channel in the open state when the system is in equilibrium is given by Boltzmann's law as

$$p = [1 + \exp(\Delta g^0/kT)]^{-1} \tag{6}$$

in which k is Boltzmann's constant and T is the absolute temperature.

If x_r is the spring's resting extension when the bundle is undisturbed, the extension of each gating spring (x) is

$$x = \gamma X + x_r \tag{7}$$

when the bundle's tip is displaced a distance X. The geometrical gain (γ) is determined by the arrangement of the gating spring within the hair bundle. If, for example, each stereociliary tip link is a gating spring, then γ is approximately equal to the ratio of the spacing between stereocilia to the height at which the displacement (X) is measured. Because the mean stereociliary spacing along the axis of stimulation is 0.95 μm and the height of the kinociliary bulb at which forces are applied is 6.7 μm, γ is about 0.14 in the bullfrog's sacculus (Howard et al., 1988).

The probability of a channel being open in the steady state is found by combining Equations 5, 6, and 7;

$$p = \{1 + \exp[-z(X - X_0)/kT]\}^{-1} \tag{8}$$

This is Equation 2 of Introduction. The single-channel gating force (z) which indicates the transducer's sensitivity to displacement, is equivalent to $\kappa_G d\gamma$ (Corey and Hudspeth, 1983b; Hudspeth, 1985a; Holton and Hudspeth, 1986). If the transduction elements are identical, then the steady-state transduction current is proportional to p and has the sigmoidal dependence on bundle displacement given by Equation 8.

The force exerted by a gating spring on its insertions is $\kappa_G(x + d/2)$ when the channel is closed and $\kappa_G(x - d/2)$ when the channel is open. The time average of the force exerted by 1 transduction element is thus

$$f = pf_o + (1 - p)f_c = \kappa_G(x + d/2) - \kappa_G dp \tag{9}$$

Because of the lever ratio (γ) between spring elongation and bundle displacement, the force exerted at the tip of the bundle (and in the direction of the bundle's deflection) by N identical transduction elements is $N\gamma f$. The steady-state force required to hold the hair bundle at position X is

$$F = K_S(X - X_S) + N\kappa_G\gamma(\gamma X + x_r + d/2) - Nzp \tag{10}$$

in which K_S is the stiffness of elastic components in parallel with the transduction elements, such as the basal tapers about which the stereocilia pivot (Crawford and Fettiplace, 1985; Howard and Ashmore, 1986), and X_S is the position that the bundle would assume in the absence of gating springs.

If we bear in mind the dependence on X of the steady-state opening probability (Equation 8), differentiation of Equation 10 with respect to X gives the bundle's stiffness,

$$K_B = K_S + N\kappa_G\gamma^2 - Nz^2p(1 - p)/kT \tag{11}$$

Thus arises Equation 1 of Introduction, in which $K_G = N\kappa_G\gamma^2$.

Preparation

Experiments were performed on saccular epithelia removed from the inner ears of bullfrogs (Rana catesbeiana) of both sexes and approximately 130 mm in length. To facilitate the subsequent detachment of the otolithic membrane, each saccular macula was treated for 2.4 ks at 21°C with subtilopeptidase BPN' (50 mg·l^{-1}; Sigma Chemical Co., St. Louis, MO) in standard frog saline solution (110 mM Na$^+$, 2 mM K$^+$, 4 mM Ca^{2+}, 118 mM Cl$^-$, 3 mM D-glucose, 5 mM HEPES at pH 7.25). The macula was secured on the bottom of a 500 μl chamber and examined under a mechanically stabilized compound microscope (UEM, Carl Zeiss, Oberkochen, FRG) with differential-interference-contrast optics and a 40×, water-immersion objective lens of numerical aperture 0.75. All experiments were performed at room temperature (18°C–22°C) on hair cells at the abneural margin of the sacculus.

Low Ca^{2+} saline solutions were identical to the standard solution except that less CaCl$_2$ was included. Gentamicin saline contained 100 μM gentamicin sulphate (Sigma Chemical Co.) added to the standard solution. Substitution of a bath solution was performed manually until an estimated 99% of the original solution was exchanged. In order to minimize damage to hair bundles, fibers were detached from kinociliary bulbs during solution changes.

Manufacture and Calibration of Fibers

Borosilicate glass rods 1.2 mm in diameter (Kimble KG-33, Garner Glass Co., Claremont, CA) were tapered to tip diameters of about 20 μm with an electrode puller. The tip of each rod was inserted normally into a molten hemisphere of the same glass adhering to an orange-hot platinum filament. As the rod was manually withdrawn from the melt, a solenoid holding the rod was activated just prior to fission of the ensuing strand of glass. The fibers so formed at the tip of the rods tapered from about 2 μm to 200 nm over their distal 100–200 μm. The fibers were shortened with iris scissors (Moria 9600, Fine Science Tools Inc., Belmont, CA) as necessary to give the desired stiffness. To increase their optical contrast, fibers were sputter-coated with a 300 nm layer of gold–palladium (Hummer VI, Anatech, Alexandria, VA).

The stiffness of the tip of a finished fiber was calibrated by two methods. In the first, a small, acrylic sphere of known weight was hung from the tip and the resulting vertical displacement (3–30 μm) was measured under a compound microscope (Howard and Ashmore, 1986). In the second, the tip's Brownian motion was measured in saline solution using the optical displacement-detection apparatus described below. By the principle of equipartition of

energy, the potential energy equals the thermal energy: $\frac{1}{2}K_F\langle X^2\rangle = \frac{1}{2}kT$, in which K_F is the stiffness of the tip of the fiber, and $\langle X^2\rangle$ is the mean-square deflection of the tip. Two factors are pertinent to the measurements of Brownian motion. First, its amplitude was easily resolved with the optical apparatus; second, most of its power lay within our recording bandwidth. The root-mean-square displacements of 2.5–5 nm measured during Brownian motion were consistent with stiffness values of 150–600 $\mu N\cdot m^{-1}$. The stiffness of each fiber was measured to an accuracy of 10%. The spectral density of the Brownian motion was well fitted in each instance by a single Lorentzian with a corner frequency of 400–2000 Hz, which corresponds to a time constant, τ_F, of 80–400 μs. The hydrodynamic drag on a fiber, $\xi_F = \tau_F K_F$, was 50–200 $nN\cdot s\cdot m^{-1}$. Measurements of Brownian motion when the tip of the fiber was attached to a hair bundle showed that the drag on the bundle, $\xi_B = 200$ $nN\cdot s\cdot m^{-1}$, exceeded that contributed by the fiber. The time constant of the fiber attached to the bundle, $\tau = (\xi_F + \xi_B)/(K_F + K_B)$, was thus about 250 μs.

Measurement and Calibration of Displacements

The image of the tip of the fiber, magnified 625×, was projected onto a pair of photodiodes (UV-140-2, EG&G Electro-Optics, Salem, MA; Figure 2A). Each photodiode's current was proportional to the intensity of the heat-filtered illuminating light, which was provided by a 100 W tungsten bulb with a stabilized, direct-current power supply. During displacement measurements, the polarizer and analyzer were removed from the optical path. The photocurrents were converted to voltages, and the differential voltage was proportional to the position of the fiber over a distance equal to the fiber's optical diameter of approximately 1 μm. The time constant of the detector's circuitry, about 10 μs, was limited by the current-to-voltage converters' 20 $M\Omega$ feedback resistors and by stray capacitance.

In order to compensate for drift in the level of illumination and for changes in contrast of the stimulus fiber, computer-controlled calibrations were interleaved with the measurements. The output of the photodiode headstage was calibrated by 20 μm displacements of the photodiodes, which were mounted on a piezoelectrical bimorph. Because the optical magnification was 625×, this calibration step corresponded to a 32 nm step in the object plane. This calibration accorded with that obtained by displacing a freely moving fiber a known distance with the piezoelectrical stimulator.

The feedback resistance of the current-to-voltage converters was chosen so that the power of Johnson (thermal) current noise was an order of magnitude smaller than that of the shot noise due to the random capture of photons by the photodiodes. Ground-borne vibrations were minimized by mounting the recording apparatus on a vibration isolation table (GH-34-ST, Newport Corp., Fountain Valley, CA) immediately above bedrock. Acoustical vibrations were reduced by enclosing the apparatus in a sound-attenuating room with a sound-transmission class of 20 dB (Kinsler et al., 1982). By these precautions we reduced the root-mean-square noise at the fiber's tip that was contributed by the apparatus to 200 pm over a frequency band of 5–1000 Hz; this is close to the photon-shot-noise limit set by the intensity of the illuminating lamp.

Mechanical Stimulation

In a measurement of a hair bundle's stiffness, the tip of a flexible, horizontally mounted glass fiber was attached to the bundle (Figure 2A) and the fiber's base was moved horizontally, perpendicular to the fiber's axis (Crawford and Fettiplace, 1985; Howard and Ashmore, 1986). Clean fibers attached firmly to the kinociliary bulb: a 1–5 μm displacement of the fiber's base was needed to break the contact. This displacement is as much as 10 times that used during the measurement of bundle stiffness.

The shank of the fiber was held in a piezoelectrical micromanipulator, which also served to move the fiber's base through calibrated displacements (Corey and Hudspeth, 1980). Both metal surfaces of each bimorph were divided into two conducting areas, and the stimulating voltage was applied to one surface on one side and to the nonopposing surface on the other. This arrangement induces the ends of each bimorph to undergo parallel displacements; as a result, a strong structure can be built with rigid bonding at both ends of each bimorph (Muralt et al., 1986). To ensure that the stimu-

lator was not excited at its lowest resonant frequency of 2 kHz, the driving signal was filtered at 800 Hz with a 16-pole Bessel fiter. The bimorph's resultant frequency response was flat up to nearly 1 kHz. The computer-generated driving signal included compensation for creep in the bimorphs (Corey and Hudspeth, 1980).

Protocol for Stiffness Measurements

In order to measure the anticipated stiffness deficit, we applied known forces directly to each hair bundle via a flexible glass fiber attached to the kinociliary bulb (Figure 2A). Using the stimulator, we moved the base of the fiber by various distances (Y_i) in both the positive and negative directions (Figure 2B). The resulting displacements (X_i) of the tip of the fiber and the adherent hair bundle were measured with the photodiode sensor. The force applied to the bundle's tip by the ith stimulus (F_i) is given by

$$F_i = K_F (Y_i - X_i) \tag{12}$$

in which K_F is the fiber's stiffness. The bundle's stiffness was calculated with the formula

$$K_i = dF_i/dX_i = (F_{i+1} - F_i)/(X_{i+1} - X_i) = K_F \{[(Y_{i+1} - Y_i)/(X_{i+1} - X_i)] - 1\} \tag{13}$$

The force pulses, 10 or 20 ms in duration, were presented every 64 ms. A stimulus run consisted of up to 32 pulses: 8 pulses increasing from zero to the maximal positive amplitude, followed by 16 pulses stepping from the largest positive to the largest negative size, concluding with 8 negative pulses decreasing in magnitude to zero. Sixteen such runs were typically averaged on-line. The amplitudes of consecutive displacements of the fiber's base increased or decreased by a constant increment, either 50 or 100 nm. In order that each response be minimally affected by prior stimuli, the pulses were kept brief and the interstep interval was 2 to 5 times the stimulus duration. The stimulus protocol of increasing and decreasing pulse sizes allowed us to confirm that hysteresis was negligible.

Microelectrode Recording, Data Collection, and Analysis

Microelectrodes were bent 0.5–1 mm from their tips (Hudspeth and Corey, 1978) and filled with 3 M KCl buffered to pH 8.5 with 10 mM glycylglycine (Sigma Chemical Co.; Thomas, 1978). Their tips, of resistance 100–300 $M\Omega$, were inserted into the apical surfaces of hair cells with the aid of Huxley-type micromanipulators (Frederick Haer & Co., Brunswick, ME). Recordings were made with a direct-coupled amplifier (Axoclamp-2A, Axon Instruments Inc., Burlingame, CA) with its capacitance compensation adjusted for a passband of 0–1000 Hz.

Under the circumstances of recording, the reversal potential for the transduction current is near 0 mV (Corey and Hudspeth, 1979b). Because the largest receptor potentials measured were about 16 mV in peak-to-peak magnitude, the driving force did not vary greatly during responses. The receptor potential could therefore be used as an index of the range of hair-bundle displacements over which the receptor current varied.

All recordings were filtered at 1 kHz with 8-pole Bessel filters, digitized on-line with a sampling interval of 500 μs, and analyzed on a computer (PDP-11/73, Digital Equipment Corp., Maynard, MA) running BASIC-23 (Indec Systems, Sunnyvale, CA). The Newton-Gauss method was used for curve-fitting (Sagnella, 1985).

References

Armstrong, C. M., and Bezanilla, F. (1974). Charge movement associated with the opening and closing of the activation gates of the Na channels. J. Gen. Physiol. 63, 533–552.

Burton, A. C. (1954). Relation of structure to function of the tissues of the wall of blood vessels. Physiol. Rev. 34, 619–642.

Corey, D. P., and Hudspeth, A. J. (1979a). Response latency of vertebrate hair cells. Biophys. J. 26, 499–506.

Corey, D. P., and Hudspeth, A. J. (1979b). Ionic basis of the receptor potential in a vertebrate hair cell. Nature 281, 675–677.

Corey, D. P., and Hudspeth, A. J. (1980). Mechanical stimulation and micromanipulation with piezoelectric bimorph elements. J. Neurosci. Meth. 3, 183–202.

Corey, D. P., and Hudspeth, A. J. (1983a). Analysis of the microphonic potential of the bullfrog's sacculus. J. Neurosci. 3, 942–961.

Corey, D. P., and Hudspeth, A. J. (1983b). Kinetics of the receptor current in bullfrog saccular hair cells. J. Neurosci. 3, 962–976.

Crawford, A. C., and Fettiplace, R. (1985). The mechanical properties of ciliary bundles of turtle cochlear hair cells. J. Physiol. 364, 359–379.

Eatock, R. A., Corey, D. P., and Hudspeth, A. J. (1987). Adaptation of mechanoelectrical transduction in hair cells of the bullfrog's sacculus. J. Neurosci. 7, 2821–2836.

Flock, Å., and Strelioff, D. (1984). Sensory hairs in the mammalian hearing organ have graded and nonlinear mechanical properties. Nature 310, 597–599.

Ford, L. E., Huxley, A. F., and Simmons, R. M. (1981). The relation between stiffness and filament overlap in stimulated frog muscle fibres. J. Physiol. 311, 219–249.

Gotte, L., Giro, M. G., Volpin, D., and Horne, R. W. (1974). The ultrastructural organization of elastin. J. Ultrastruct. Res. 46, 23–33.

Holton, T., and Hudspeth, A. J. (1986). The transduction channel of hair cells from the bull-frog characterized by noise analysis. J. Physiol. 375, 195–227.

Howard, J., and Ashmore, J. F. (1986). Stiffness of sensory hair bundles in the sacculus of the frog. Hearing Res. 23, 93–104.

Howard, J., and Hudspeth, A. J. (1987). Mechanical relaxation of the hair bundle mediates adaptation in mechanoelectrical transduction by the bullfrog's saccular hair cell. Proc. Natl. Acad. Sci. USA 84, 3064–3068.

Howard, J., Roberts, W. M., and Hudspeth, A. J. (1988). Mechanoelectrical transduction by hair cells. Annu. Rev. Biophys. Chem. 17, in press.

Hudspeth, A. J. (1982). Extracellular current flow and the site of transduction by vertebrate hair cells. J. Neurosci. 2, 1–10.

Hudspeth, A. J. (1983). Mechanoelectrical transduction by hair cells in the acousticolateralis sensory system. Annu. Rev. Neurosci. 6, 187–215.

Hudspeth, A. J. (1985a). Models for mechanoelectrical transduction by hair cells. In Contemporary Sensory Neurobiology, M. J. Correia and A. A. Perachio, eds. (New York: Alan R. Liss), pp. 193–205.

Hudspeth, A. J. (1985b). The cellular basis of hearing: the biophysics of hair cells. Science 230, 745–752.

Hudspeth, A. J., and Corey, D. P. (1977). Sensitivity, polarity, and conductance change in the response of vertebrate hair cells to controlled mechanical stimuli. Proc. Natl. Acad. Sci. USA 74, 2407–2411.

Hudspeth, A. J., and Corey, D. P. (1978). Controlled bending of high-resistance glass microelectrodes. Am. J. Physiol. 234, C56–C57.

Huxley, A. F., and Simmons, R. M. (1971). Proposed mechanism of force generation in striated muscle. Nature 233, 533–538.

Kinsler, L. E., Frey, A. R., Coppens, A. B., and Sanders, J. V. (1982). Fundamentals of Acoustics, Third Edition (New York: John Wiley & Sons, Inc.), pp. 303–306.

Lewis, R. S., and Hudspeth, A. J. (1983). Voltage- and ion-dependent conductances in solitary vertebrate hair cells. Nature 304, 538–541.

Muralt, P., Pohl, D. W., and Denk, W. (1986). Wide-range, low-operating-voltage, bimorph STM: application as potentiometer. IBM J. Res. Dev. 30, 443–450.

Ohmori, H. (1984). Mechanoelectrical transducer has discrete conductances in the chick vestibular hair cell. Proc. Natl. Acad. Sci. USA 81, 1888–1891.

Ohmori, H. (1985). Mechano-electrical transduction currents in isolated vestibular hair cells of the chick. J. Physiol. 359, 189–217.

Ohmori, H. (1987). Gating properties of the mechano-electrical transducer channel in the dissociated vestibular hair cell of the chick. J. Physiol. 387, 589–609.

Pickles, J. O., Comis, S. D., and Osborne, M. P. (1984). Cross-links between stereocilia in the guinea pig organ of Corti, and their possible relation to sensory transduction. Hearing Res. 15, 103–112.

Sagnella, G. A. (1985). Model fitting, parameter estimation, linear and non-linear regression. Trends Biochem. Sci. 10, 100–103.

Thomas, R. C. (1978). Ion-Sensitive Intracellular Microelectrodes (London: Academic Press, Inc.), p. 19.